# Modulating carboxymethylcellulose-based hydrogels with superior mechanical and rheological properties for future biomedical applications

*N. A. Dahlan[1], S. Y. Teow[2], Y. Y. Lim[1], J. Pushpamalar[1,3*]*

[1]School of Science, Monash University Malaysia, Jalan Lagoon Selatan, 47500 Bandar Sunway, Selangor, Malaysia
[2]Department of Medical Sciences, School of Healthcare and Medical Sciences, Sunway University, Jalan Universiti, 47500 Bandar Sunway, Selangor, Malaysia
[3]Monash-Industry Palm Oil Education and Research Platform (MIPO), Monash University Malaysia, Jalan Lagoon Selatan, 47500 Bandar Sunway, Selangor, Malaysia

**Abstract.** Herein, a grafted copolymer composed of carboxymethylcellulose (CMC) and polyethylene-glycol-aminated (PEG-NH$_2$) was successfully synthesized via a facile ionic interaction and scalable route in the presence of EDC/NHS (*N*-ethyl-*N'*-(3-dimethylaminopropyl)carbodiimide/*N*-hydroxysuccinimide) activators. From Fourier transform infrared (FT-IR) spectroscopy, the absorption peak at 1652 cm$^{-1}$ corresponded to –NH groups of PEG-NH$_2$. After grafting, the grafted CMC-PEG was characterized for surface morphology, crystallinity, functional groups determination, and thermal analysis. No cytotoxicity effect was observed in normal human dermal fibroblasts (NHDFs) cells following exposure to the grafted CMC-PEG up to 2 mg/ml. The rheological studies suggested that the optimized 10% (w/v) grafted CMC-PEG hydrogels crosslinked with 5% (w/v) citric acid (CA) exhibited better mechanical properties compared to the non-grafted CMC. This work highlights the characterizations of grafted CMC-PEG and demonstrates the potential of grafted CMC-PEG hydrogels crosslinked with CA for advanced 3D-bioprinting or as injectable hydrogels in various biomedical applications such as tissue engineering, wound dressing materials, and drug delivery systems.

*Keywords: rheology, carboxymethylcellulose, grafted copolymer, hydrogel, normal human dermal fibroblasts (NHDFs)*

## 1. Introduction

Polymers modification is an exciting field of study, especially in applied science research. Modification of polymers to produce new polymeric materials through methods such as physical and chemical processes have been extensively studied over the past few decades [1]. The physical process involves blending, irradiation, and oxidation with gases is a direct method to produce new polymeric materials. However, it was reported that the physical blending of two polymers with distinct properties could result in undesirable mechanical strength and water absorption [2, 3]. On the other hand, chemically modified polymer through techniques such as grafting has advantages over several physical processes. This includes controllable and specific binding of interest polymer chains through the formation of covalent bonds between chemically reactive functional groups [4]. Carboxymethylcellulose (CMC) is a low-cost natural polysaccharide with a wide range of applications. CMC is commonly used as a thickener, viscosity modifier, and water retention agent in the food industry as well as textile, flocculation, and oil drilling industries. CMC is known to be non-cytotoxic,

biocompatible, and biodegradable polysaccharides. Therefore, research on CMC had branched out to more advanced fields such as heavy metals/dyes adsorption, drug delivery systems, and tissue engineering [5–7]. Polyethylene glycol (PEG) is a biocompatible, hydrophilic, and non-immunogenic synthetic polymer. PEG was reported to respond significantly to the change of pH by swelling and shrinking to increase tissue formation during the early wound healing stage and leads to the release of growth factors embedded in the scaffold matrix. Besides, most PEGs with molecular weight less than 1000g/mol can be removed rapidly from the body system, thus contributes to its wide usage in biomedical applications such as drug delivery systems and scaffolds for tissue engineering [8]. According to Ghorpade *et al.* [9], the reactive hydroxyl end terminal (–OH) of PEG can be easily activated and replaced with different functional groups such as azide, carboxyl acid, thiol, and amine. Functionalization of synthetic polymers diversified their potentials as biomaterials in the biomedical field.

The advantage of CMC to develop biomaterials originates from its abundant functional groups such as hydroxyl (–OH) and carboxylate (–COO⁻) groups. Therefore, copolymerization of CMC as the main backbone with different polymers to improve its physical and chemical properties are feasible with minimal changes to its nature. Kumar and Negi [10] reported the synthesis of CMC-*graft*-poly(sodium 1-hydroxyacrylate) (CMC-*g*-PnaHA). The grafted copolymers demonstrated 427 times higher water uptake capacity and better thermal stability compared to CMC and PnaHA, respectively. In another study by Alange *et al.* [11], polyacrylamide-*graft*-CMC (PAAm-*g*-CMC) showed promising potential as microspheres carriers to deliver capecitabine for the colon drug delivery system. Dahlan *et al.* [12] reported the synthesis of CMC-*graft*-polyvinyl alcohol (CMC-*g*-CMPVA) with smart swelling behavior in different pH environments and biocompatible to living cells.

Most hydrogels are promising candidates for various biomedical applications due to their biocompatible nature and could provide a 3D environment with a high water content to support cell regeneration [13]. Furthermore, hydrogels are an appealing material for tissue engineering due to their structural similarity to the extracellular matrix (ECM) of tissues and can be applied in a minimally invasive manner. Besides,

the fabrication of hydrogels can be done under relatively mild conditions [14]. Many studies reported the potential of CMC-based hydrogels for various biomedical applications ranging from drug carriers for drug delivery, wound dressing materials to injectable hydrogels and scaffolds for tissue engineering [15–19].

In this work, grafted CMC-PEG was synthesized through two simple reaction steps represented in Figure 1. The structural properties of the synthesized grafted CMC-PEG were characterized by Fourier transform infrared (FTIR), carbon and proton nuclear magnetic resonance (NMR) to confirm the grafting of PEG-NH$_2$ to CMC. Furthermore, the surface morphology, crystallinity, thermal behavior, and cytotoxicity of the synthesized product were also studied. The rheological study was performed to study the potential of grafted CMC-PEG hydrogel as hydrogel scaffolds, injectable hydrogels, and hydrogels inks in 3D-printing for future biomedical applications.

## 2. Experimental
### 2.1. Materials
Carboxymethyl cellulose, sodium salt (CMC) ($M_w$ = 135 000 g/mol, degree of substitution ($DS$) = 0.85), triethylamine, sodium carbonate (Na$_2$CO$_3$) and *N*-hydroxysuccinimide (NHS) were purchased from Nacalai Tesque, Japan. *N*-ethyl-*N'*-(3-dimethylaminopropyl)carbodiimide (EDC), ρ-toluenesulfonyl chloride were purchased from Sigma-Aldrich, USA. Polyethylene glycol ($M_w$ = 4000 g/mol), sodium chloride (NaCl), and glycine were supplied by Merck, Germany. Dichloromethane (DCM), magnesium sulfate anhydrous (MgSO$_4$), potassium chloride (KCl), citric acid, and hydrochloric acid (HCl) were purchased from Friendemann Schmidt, Australia, while 30% ammonia solution, potassium dihydrogen phosphate (KH$_2$PO$_4$) and 2-propanol were purchased from R&M Chemicals, United Kingdom. Ninhydrin reagent was obtained from Fisher Scientific, United States (US) while disodium hydrogen phosphate (Na$_2$HPO$_4$) was supplied by HmBG Chemicals, Germany. MTS 3-(4,5-dimethylthiazol-2-yl)-5-(3-carboxymethoxyphenyl)-2-(4-sulfophenyl)-2H-tetrazolium was purchased from Promega Corporation, USA. Fibroblast basal medium, fetal calf serum (FCS), human basic fibroblast growth factor (hbFGF), and insulin solution were purchased from PromoCell GmbH, Heidelberg, Germany. Dichloromethane was dried over

magnesium sulfate while ρ-toluenesulfonyl chloride was re-crystallized using acetone before use.

## 2.2. Method

### 2.2.1. Synthesis of PEG-NH$_2$

The modification of hydroxyl groups (–OH) of PEG with amine groups (–NH$_2$) groups was performed according to Cameron *et al*. [20] with modification. Briefly, PEG (10 g) was dissolved in 100 ml of dry dichloromethane. After the addition of triethylamine (7.5 ml), the solution was cooled to 0 °C. Then, *p*-toluenesulfonyl chloride (5 g) was added and stirred overnight at room temperature. The residue was filtered from the solution, and the filtrate was washed using a separatory funnel with 30 ml of 1 M sodium carbonate solution to remove unreacted *p*-toluenesulfonyl chloride. The bottom layer was extracted for subsequent neutralization. Then, 30 ml of 10% HCl for neutralizing the filtrate was added to the bottom layer. The bottom layer containing PEG-tosylate was extracted while the upper layer was removed. The remaining solvent was then removed by rotary evaporation. Next, the yellow product (10 g) was dissolved in 25% aqueous ammonia solution (150 ml), and the reaction mixture was vigorously stirred for 3 days at room temperature. The reacted mixture was left overnight to evaporate the ammonia. The basic solution containing remaining ammonia was extracted three times with DCM using a separatory funnel, and finally, the DCM was removed by rotary evaporation.

### 2.2.2. Grafting of PEG-NH$_2$ onto CMC

For the synthesis of grafted CMC-PEG, 2% (w/v) CMC and PEG-NH$_2$ were separately dissolved in distilled water. Subsequently, the activating agents of EDC and NHS (2:1) were added to the CMC solution to activate the reaction, followed by the addition of dissolved PEG-NH$_2$. In this study, EDC coupled with NHS was used to activate the carboxyl groups of CMC to form a stable amide bond with primary amines of PEG-NH$_2$ [21]. The final concentration of the reaction mixture was CMC (0.07 mM), PEG-NH$_2$ (2.50 mM), EDC (9.66 mM), and NHS (6.52 mM). The reaction took place at room temperature for 24 hours by stirring in a sealed beaker. To remove unbound PEG-NH$_2$, the solution was dialyzed against distilled water overnight. Finally, the product was dried to constant weight. The grafted CMC-PEG solid was grounded and sieved through 150 μm and stored

in a desiccator for subsequent analyses. The percentage yield of the final was calculated by Equation (1):

$$\text{Percentage yield [\%]} = \frac{W_f}{W_c} \cdot 100 \tag{1}$$

where $W_f$ denotes the weight of grafted CMC-PEG and $W_c$ represents the initial weight of CMC.

### 2.2.3. Degree of grafting

The degree of grafting was determined by ninhydrin assay. First, approximately 100 mg of grafted CMC-PEG was heated with the ninhydrin reagent (2% (w/v) in 2-propanol) at 100 °C for 15 minutes. The PEG-NH$_2$ sample was considered as the control. The solution was cooled at room temperature, and the optical absorbance was recorded at 570 nm using a spectrophotometer. The amount of –NH$_2$ groups was determined from a standard curve of glycine concentration versus absorbance. The degree of grafting was calculated by Equation (2):

$$\text{Degree of grafting [\%]} = \frac{NH_i - NH_f}{NH_i} \cdot 100 \tag{2}$$

where $NH_i$ and $NH_f$ represent the amount of free amine groups before and after grafting.

### 2.2.4. Characterization

The surface morphology of the synthesized grafted CMC-PEG was examined on a Hitachi SU8010 field emission electron microscope (FESEM). The sample was sputter-coated with platinum after mounting on double-sided carbon tape. The infrared spectra of PEG, PEG-NH$_2$, CMC, and grafted CMC-PEG were taken in the range of 400–4000 cm$^{-1}$ using Spectrum-Two FT-IR spectrophotometer, Perkin Elmer, Inc. XRD patterns of PEG, PEG-NH$_2$, CMC, and grafted CMC-PEG powdered samples were recorded in the range of 5–60° at ambient temperature on BRUKER D8 Discover X-ray Diffraction system. Percentage crystallinity was calculated using Equation (3) [22]:

$$\text{Percentage crystallinity [\%]} = \frac{A_c}{A_c + A_a} \cdot 100 \tag{3}$$

where $A_c$ represents the area of the crystalline peak while $A_a$ is the area of the amorphous peak. Molecular weights and polydispersities of PEG-NH$_2$ and grafted CMC-PEG were determined by gel permeation chromatography (GPC, Tosoh EcoSEC HLC-8320GPC) equipped with both refractive index

(*RI*) and ultraviolet (UV detection, λ = 280 nm) detectors using Tosoh alpha 4000 and 2000 columns. The solvent and mobile phase was water containing 0.1 M $NaNO_3$ and 0.1 M $NaHCO_3$ with a flow rate of 1 ml/min. The calibration curves were obtained using 10× low dispersity PEG/PEO standards (PEG/PEO: 615–$1.38 \cdot 10^6$ g/mol, $R^2$ = 0.9995). ^{1}H NMR (nuclear magnetic resonance) of grafted CMC-PEG was recorded at 30 °C in $D_2O$ using BRUKER 500 MHz FT-NMR with a relaxation delay time of 1 second. [13]C cross-polarization magic angle spinning (CPMAS) was recorded using a Bruker BioSpin GmbH operating at 75.44 MHz. In CPMAS experiment, the sample was spun at 10 kHz. For differential scanning calorimetry, approximately 5 mg of CMC, PEG, $PEG-NH_2$, and grafted CMC-PEG powdered samples were analyzed by DSC Q100 in a platinum crucible scan with a scan speed of 20 °C/min over a temperature range of –50 to 200 °C under constant nitrogen. The samples were pre-dried in the oven overnight prior to the analysis. The following protocol was used for each sample: equilibrate at –50 °C and isothermal for 1 min, heating to 200 °C and isothermal for 1 min, cooling to –50 °C and isothermal for 1 min, and finally reheating to 200 °C. Data was collected from the second heating curve. The thermograms of CMC, PEG, $PEG-NH_2$, and grafted CMC-PEG were obtained using TGA Q500 V6.7 Build 203 device. Approximately 5 mg samples were analyzed with temperatures ranging from 25 to 700 °C under nitrogen.

### 2.2.5. Cell cytotoxicity study
*Cell culture*
Normal human dermal fibroblasts (NHDFs) was cultured in fibroblast basal medium (FBM) supplemented with 2% (v/v) fetal bovine serum (FBS), 1 ng/ml basic fibroblast growth factor (hbFGF), 5 µg/ml insulin solution, 100 U/ml penicillin and 100 µg/ml streptomycin in a 25 cm² cell culture flask. The NHDFs cells were then incubated in a humidified atmosphere (95%) containing 5% $CO_2$ at 37 °C. The culture medium was changed every three days.

*Quantitative cell viability MTS assay*
The cytotoxicity of grafted CMC-PEG at different concentrations was determined using MTS colorimetric assay. Before the experiments, 10 mg of powdered grafted CMC-PEG were sterilized by UV light for 60 min, followed by the addition of 500 µl of sterile water, and incubated in the oven at 80 °C until dissolution. The stock polymer solution with 10 mg/ml concentration was achieved by adding 500 µl of FBM media to the dissolved polymer solution. Subsequently, test samples containing grafted CMC-PEG with concentrations ranging from 0.00001 to 10 mg/ml were prepared by diluting the stock solution. NHDFs cells with a density of $2.5 \cdot 10^4$ cells/ml were seeded onto a 96-well sterile tissue culture plate (TCP) containing 100 µl FBM and kept in the incubator at 37 °C for 24 h. Subsequently, the FBM medium in each NHDFs seeded well was replaced with 100 µl of the prepared grafted CMC-PEG at different concentrations ($CP_e$). Furthermore, NHDFs seeded with FBM acted as the control ($NHDF_c$) while non-seeded wells with either grafted CMC-PEG solutions with different concentrations ($CP_b$) or FBM medium ($F_b$) served as the blank. The prepared TCP was incubated for 24 h. At the end of the time-point, 10 µl of MTS solution was added to the wells, followed by incubation at 37 °C for 3 h. Then, the optical density (*OD*) values were measured at a wavelength of 490 nm using a Microplate reader. The relative cell viability was calculated by Equation (4):

$$\text{Cell viability [\%]} = \frac{OD\,CP_e - OD\,CP_b}{OD\,NHDF_c - OD\,F_b} \cdot 100 \quad (4)$$

### 2.2.6. Grafted CMC-PEG hydrogel preparation
In this study, 10% (w/v) grafted CMC-PEG was prepared by dissolving the polymer in distilled water. The polymer solution was incubated in the oven at 80 °C to ensure complete dissolution. For the crosslinking of hydrogels with citric acid (CA), the dissolved grafted CMC-PEG was crosslinked with 5, 10, and 15% (w/v) of CA, indicated by 10% CMC-$PEG_5$, 10% CMC-$PEG_{10}$, and 10% CMC-$PEG_{15}$, respectively before the analysis. The hydrogels were incubated in the oven at 37 °C overnight during the crosslinking process. On the other hand, 2.5% (w/v) CMC was dissolved at room temperature. Then, the same steps were repeated for preparing 2.5% (w/v) cross-linked with 5, 10 and 15% (w/v) of CA denoted as 2.5% CMC5, 2.5% $CMC_{10}$ and 2.5% $CMC_{15}$, respectively.

### 2.2.7. Rheology analysis
Rheology measurements were performed at 25 °C on an Anton Paar MCR 302 rheometer. The measurements were performed using a sand blasted-type

geometry (25 mm in diameter). The storage modulus ($G'$) and loss modulus ($G''$) of materials were measured in oscillatory mode at 25 °C. For amplitude sweep measurement, the hydrogel materials were tested for strain values of 0.01 to 1000% by keeping the angular frequency constant at 10 Hz. In the frequency sweep measurement, the hydrogel materials were tested from 0.1 to 100 rad/s frequency range by keeping constant the shear strain constant at 0.5%.

### 2.2.8. Statistical analysis

Data were analyzed by one-way analysis of variance (ANOVA) using GraphPad Prism Version 8.1.2 for Windows (GraphPad Software, Inc.) and presented as mean ± standard deviation for triplicates with $p < 0.05$.

## 3. Results and discussion
### 3.1. Synthesis of grafted CMC-PEG

In this study, the amine groups of functionalized PEG-NH$_2$ were grafted to the reactive carboxyl groups on the backbone of CMC via a 'grafting to' approach. In this approach, new properties will be introduced to the newly grafted product while maintaining the desirable properties of each polymer substrate [23, 24]. First, PEG-NH$_2$ was modified through asymmetric activation of symmetrical PEG. PEG-tosylate was then synthesized as a precursor before the amination process, as shown in Figure 1a. Tosylate groups are excellent candidates for substitution reactions to enable the conversions of different functional groups [25]. Formation of grafted CMC-PEG was achieved

through coupling reaction of EDC/NHS. In this case, EDC activated the carboxyl group of CMC to form an unstable amine-reactive intermediate followed by coupling NHS that rearranged the intermediate into a more stable amine-reactive ester. A stable amide bond was then created between CMC and PEG-NH$_2$ to form grafted CMC-PEG [21, 26]. Based on the grafting reaction scheme of grafted CMC-PEG illustrated in Figure 1(b), the grafting of PEG-NH$_2$ could be alternately random on the CMC backbone.

According to Kumar *et al.* [27], ninhydrin causes oxidative deamination of –NH$_2$ releasing ammonia (NH$_3$) followed by condensation of reduced ninhydrin to form colored substances. Therefore, the degree of PEG-NH$_2$ grafted onto the CMC backbone was investigated using the ninhydrin assay. A similar approach was used by Baharifar *et al.* [28] to measure the amount of free amines of deacetylated chitosan conjugated to PEG. The free amine groups of PEG-NH$_2$ were measured using ninhydrin method before and after the grafting process. It was found that 71% of PEG-NH$_2$ was successfully grafted to CMC. Meanwhile, a percentage yield of 177% was obtained after the grafting of PEG-NH$_2$ to CMC. The high yield indicates an ideal CMC-PEG grafting approach for large-scale production of polymeric biomaterials.

### 3.2. Field emission electron microscope (FESEM)

Figure 2a shows the granule morphology of grafted CMC-PEG. The granular appearance of grafted
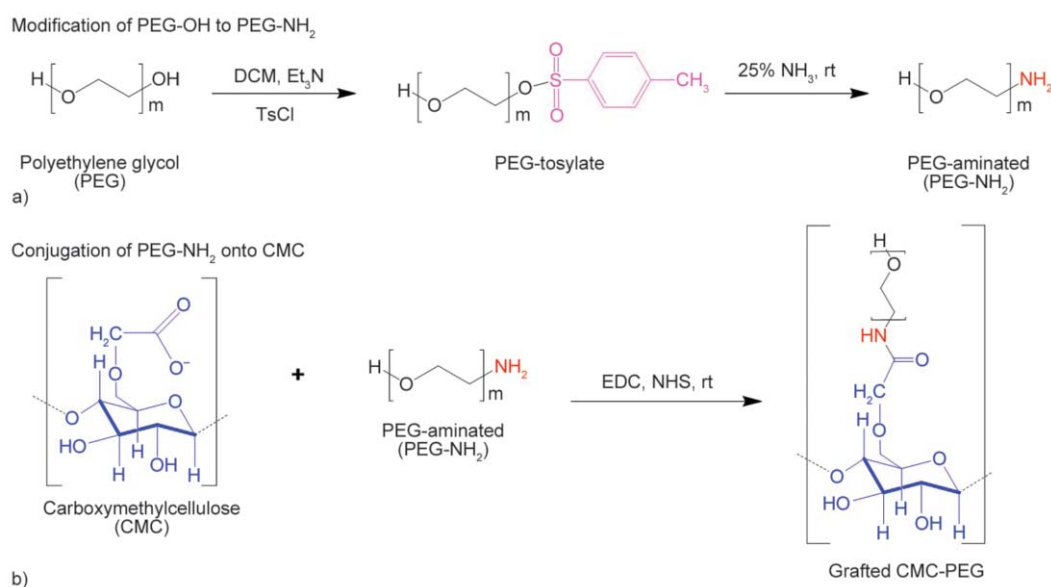


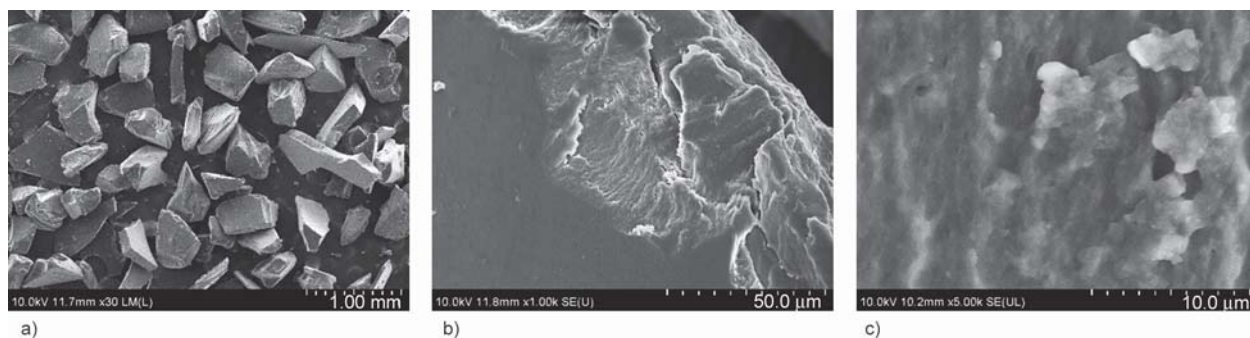**Figure 1.** Schematic representations of (a) modification of PEG-OH to PEG-NH$_2$ and (b) the grafting of PEG-NH$_2$ to CMC.

**Figure 2.** Surface morphology of grafted CMC-PEG at (a) ×30, (b) ×1000 and (c) ×5000 magnifications.

CMC-PEG at higher magnification showed a smooth surface with rough edges, as shown in Figure 2b and 2c.

## 3.3. Fourier transform infrared (FT-IR) and X-ray diffraction (XRD) analyses

Fourier transform infrared spectroscopy was used to characterize and identify the functional groups of PEG, PEG-NH$_2$, CMC, and grafted CMC-PEG, as shown in Figure 3a. The infrared spectrum of CMC showed a broad spectrum at 3288 cm$^{-1}$, which represents the –OH stretching of non-substitute hydroxyl groups of the cellulose. An absorption band at 2886 cm$^{-1}$ exhibited –CH stretching vibration. According to the literature, the bands caused by –CO stretching of the ether linkage [1,4-β-D-glucoside] or the ether group outside and inside the ring of cellulose carboxymethylation can be detected 1024 cm$^{-1}$ [12]. The absorption bands at 1590, 1416, and 1322 were attributed to carbonyl stretch of –COO$^-$, the –CH$_2$ bending of scissoring type and –CO vibration, respectively. The spectrum of PEG exhibited the characteristic bands attributed to C–H bonds at 2750 cm$^{-1}$ stretching vibration. The broad band centered at 3480 cm$^{-1}$ was assigned to

the –OH stretching. In addition to that, the band around 1100–1000 cm$^{-1}$ was assigned to –COC bonds. After modification with amine groups (NH$_2$), the most significant differences can be detected at specific regions ranges from 4000–2500 and 1800–1600 cm$^{-1}$ as illustrated by the PEG-NH$_2$ spectrum. The band centered at 3492 cm-1 attributable to –NH2 asymmetric and symmetric stretching. Furthermore, a peak located at 1652 cm$^{-1}$ was assigned to the primary –NH$_2$ group introduced after the modification as shown in Figure 3b. The grafted CMC-PEG exhibited an absorption band at 2874 cm$^{-1}$ corresponding to the –CH functional groups. Characteristic bands of –OH and –NH at 3504 and 1656 cm$^{-1}$, indicating that the grafting of PEG-NH$_2$ to CMC was successful, as evidenced by the formation of an amide bond. The absorption bands at 1462 and 1354 were attributed to the –CH$_2$ bending of scissoring type and –CO vibration, respectively. An absorption band at 1108 cm$^{-1}$ was assigned to the –COC functional groups.

The diffraction patterns of PEG, PEG-NH$_2$, CMC, and grafted CMC-PEG are shown in Figure 4. The X-ray diffractogram of PEG showed diffraction peaks at 13.55, 19.15, 23.27, 26.26, and 27.04° with
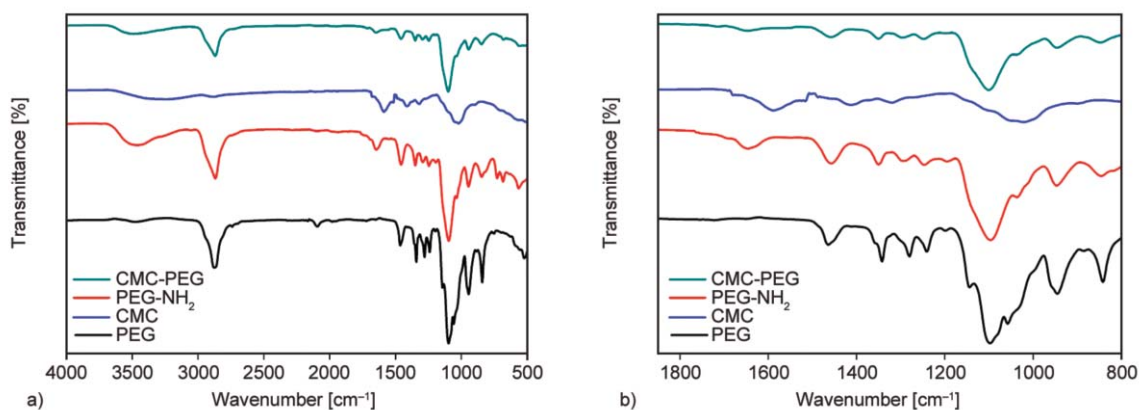


**Figure 3.** FTIR spectra of PEG, PEG-NH$_2$, CMC, and grafted CMC-PEG at (a) 400–4000 cm$^{-1}$ and (b) 850–1850 cm$^{-1}$.
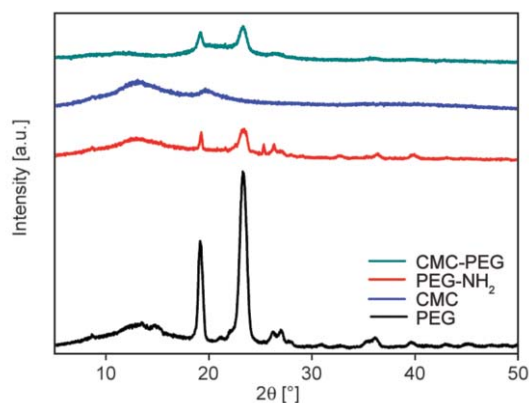
**Figure 4.** X-ray diffractograms of PEG, PEG-NH$_2$, CMC, and grafted CMC-PEG.

a percentage crystallinity of 97.1%. These are typical peaks for PEG as reported in the literature. Therefore, this indicates the PEG used in this study is of a pure form [29]. Comparing with PEG, the intensity of peaks at 2θ = 19.23 and 23.42° reduced significantly in the XRD spectrum of PEG-NH$_2$. Furthermore, the position of peaks at 2θ = 13.55, 26.26 and 27.04° have shifted to 13.02, 25.30 and 26.32°, and the percentage crystallinity reduced significantly to 81.1%. According to the literature, the functionalization of PEG with –NH$_2$ disrupts intermolecular hydrogen bonds leading to lower crystallinity [30]. CMC, having an amorphous nature, shows broad diffraction peaks at 2θ = 13.09 and 19.65° with 53.3% crystallinity. In contrast, the X-ray diffractogram of grafted CMC-PEG revealed that the crystalline domain anticipated from the presence of PEG-NH$_2$ with well-defined diffraction peaks and reduced intensities at 19.13, 23.31 and 26.63°. This indicates the successful grafting of PEG-NH$_2$ to the CMC backbone. A broad peak was also detected at 2θ = 11.66°. The results demonstrated the semi-crystalline nature of grafted CMC-PEG indicated by the mixture of crystalline and amorphous domains. Badwaik *et al*. [31] reported the disruption of the semi-crystalline nature of carboxymethyl xanthan gum with acrylamide (CMXG-*g*-PAAm). Similarly, Yang *et al*. [32] reported a decrease in crystallinity of carboxymethyl β-cyclodextrin-*grafted*-carboxymethyl chitosan. Our study found that the percentage crystallinity of grafted CMC-PEG (54.2%) was significantly lower than PEG-NH$_2$, yet comparable to the CMC. The formation of covalent bonds between the functionalized polymer and the main polymer chain (the backbone) could affect the chain arrangement, hence reducing the crystallinity [33].

### 3.4. Molecular weight analysis

The molecular weight and polydispersity index of PEG-NH$_2$ and grafted CMC-PEG obtained from GPC analysis are tabulated in Table 1. The amination of PEG to PEG-NH$_2$ exhibited a low polydispersity index (*PDI* = 1.179) with uniform polymer chains. After the grafting process, the GPC trace of grafted CMC-PEG shifted towards higher molecular weight regions with lower elution time. As a result, the molecular weight ($M_w$) of grafted CMC-PEG (572 034 g/mol) increased significantly compared to the $M_w$ of CMC (135 000 g/mol) after being grafted with PEG-NH$_2$. The exceptional $M_w$ and wide *PDI* of grafted CMC-PEG could be due to the effects of polymer branching, length, and grafting flexibility [34]. Moreover, the high $M_w$ of grafted CMC-PEG supported our calculated percentage yield of 177% mentioned in Section 3.1. Ciftci [35] reported a similar observation through the synthesis of poly(styrene-*graft*-poly(ethylene glycol) methacrylate) (PS-*g*-PEGMA).

### 3.5. Nuclear magnetic resonance (NMR)

As shown in Figure 5a, the structure of PEG-NH$_2$ was confirmed using ^{1}H NMR. Chemical shift at 2.26 ppm corresponded to the –NH$_2$ groups of PEG-NH$_2$. On the other hand, the shift at 3.57 ppm was the proton signals from the oxyethylene chains of PEG block (–CH$_2$CH$_2$O–) [36]. Veeramachineni *et al*. [37] confirmed the structure of carboxymethylcellulose synthesized from sago biomass through the appearance of chemical shifts at 3 and 4 ppm corresponded to the H1 and H2 of the glucose units, respectively. The H3–6 protons in the glucose units appeared between 4 to 4.5 ppm. Finally, the peaks appearing between 3.8 to 4.4 ppm were assigned to the methylene protons in the substituted carboxymethyl groups. Meanwhile, ^{1}H NMR spectrum of grafted CMC-PEG in D$_2$O is shown in Figure 5b. The sharp peak at 3.65 ppm was assigned to –CH$_2$CH$_2$O– chains of PEG. Similarly, the proton signals of CMC backbone related to H2 to H6 in an anhydroglucose unit and

**Table 1.** GPC data obtained for PEG-NH$_2$ and grafted CMC-PEG.

| Sample | $M_n$ [g/mol] | $M_w$* [g/mol] | *PDI* ($M_w/M_n$) |
|---|---|---|---|
| PEG-NH$_2$ | 2 592 | 3 056 | 1.179 |
| Grafted CMC-PEG | 226 287 | 572 034 | 2.528 |

*theoretical $M_w$ of PEG and CMC were 4000 g/mol and 135 000 g/mol, respectively.
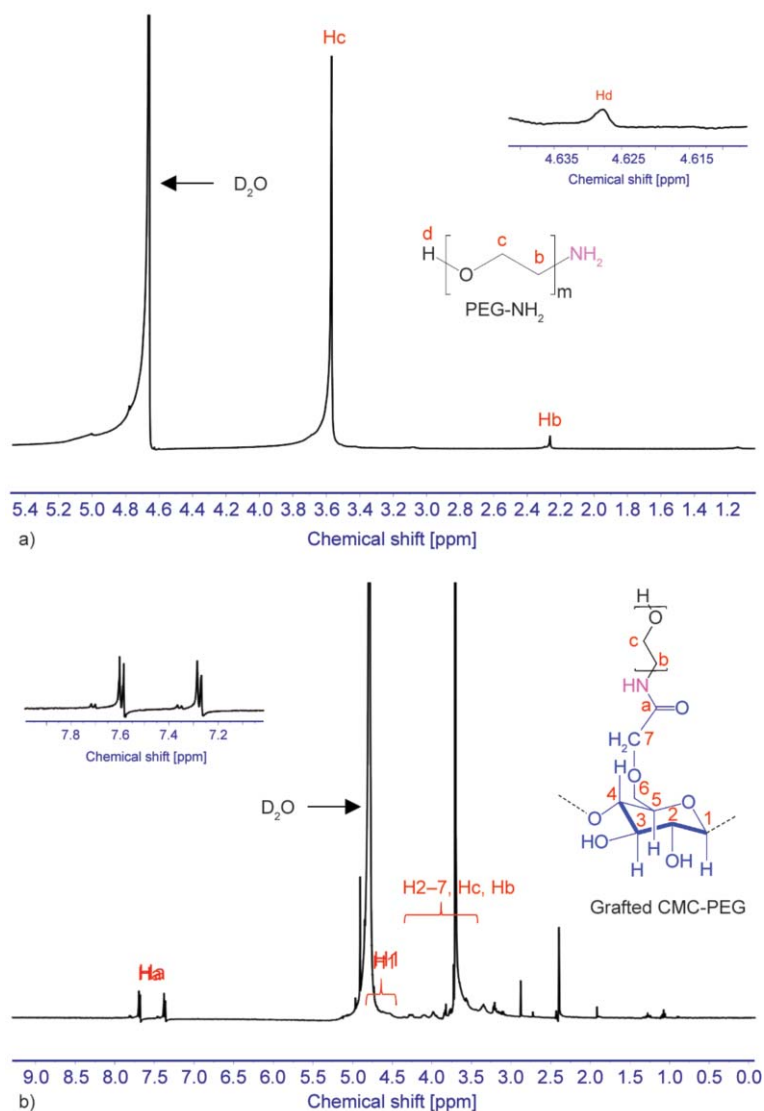
**Figure 5.** ¹H NMR of (a) PEG-NH₂ and (b) grafted CMC-PEG.

methylene protons in the substituted carboxymethyl groups appeared as broad regions between 3.60 to 4.23 ppm [38, 39]. The grafting of PEG-NH₂ onto the CMC chain was confirmed through the proton on the amide group with characteristic peaks that appeared between 7.31 to 7.71 ppm. A study by Li *et al*. [40] observed similar peaks within the same region, to confirm the conjugation of folate to carboxymethyl chitosan through polyethylene glycol spacer (CMCS-PEG-FA).

Figure 6 shows the solid-state ¹³C CPMAS NMR of grafted CMC-PEG. In the ¹³C CPMAS NMR spectrum, the six carbon atoms in the CMC glucose units appeared within 50–100 ppm. The peaks at 100.21, 94.24, and 70.76 ppm were assigned to C1, C4 and overlapping of C2, C3, C5 and C7 of the CMC. The signal at 58.62 ppm was assigned to C6 [41–43]. On the other hand, the presence of PEG was identified
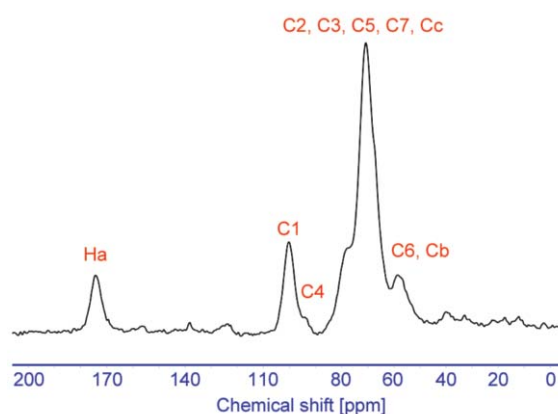


**Figure 6.** ¹³C CPMAS NMR of grafted CMC-PEG.

through the appearance of peaks at 70.76, and 58.62 ppm corresponds to the Cc and Cb. The signal at 174 ppm was specific to the amide bond due to the reaction between the –NH₂ groups of PEG-NH₂ and –COOH groups of CMC. The presence of these

signals indicated the successful formation of grafted CMC-PEG.

## 3.6. Thermal analysis

Herein, the thermal properties of PEG, PEG-NH$_2$, CMC, and grafted CMC-PEG were studied by DSC and TGA, as shown in Figure 7. The DSC thermogram of CMC showed in Figure 7a indicates that due to the amorphous state of CMC, it did not show any prominent peak after heating to 200 °C. According to the literature, the melting temperature of CMC was observed around 315 °C [44]. After PEG modification of the –OH end terminal to –NH$_2$, it was observed that the endothermic peak that corresponds to
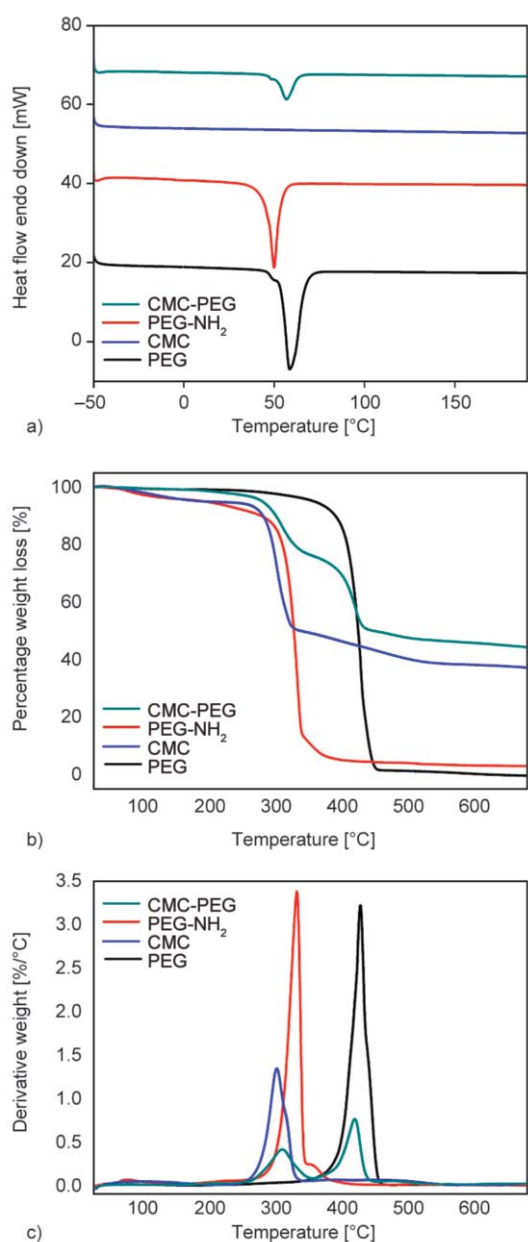
melting temperature decreased significantly to 49.91 °C. The thermal property of grafted CMC-PEG (Melting temperature, $T_m$ = 56.80 °C) indicates that the product is semi-crystalline. The enthalpy change ($\Delta H_m$) of PEG, PEG-NH$_2$, and grafted CMC-PEG are tabulated in Table 2. This concludes that $\Delta H_m$ decreased due to the –OH end terminal modification and grafting process, resulting in a reduced crystallinity of grafted CMC-PEG. This result is in line with the findings of XRD in Figure 3b.

Thermogravimetric (TGA) and derivative thermogravimetric analyses (DTG) were conducted to investigate the thermal behavior such as decomposition temperature of CMC, PEG, PEG-NH$_2$, and grafted CMC-PEG, their percentage of residue, and thermal stability (Figure 7b, 7c and Table 2). The thermal decomposition of PEG started around 355 °C and decomposed rapidly at 427.97 °C. As PEG has a simple linear chain, the thermal decomposition was assumed to occur at both –C–O and –C–C bonds of the polymer chain [45]. Interestingly, the amination of PEG to form PEG-NH$_2$ exhibited a lower decomposition temperature of 331.90 °C. The intermolecular hydrogen bond between –OH groups is stronger than the one with amine (–NH$_2$) groups, which attributes to the lower decomposition temperature [46, 47]. CMC showed a significant weight loss of 5.4% at low temperature due to the loss of water molecules. The second weight loss was then observed around 301 °C, due to the elimination of $CO_2$ from the decomposition of the hydrocarbon backbone of the polysaccharides. On the other hand, a loss in weight was observed in two stages for grafted CMC-PEG. The first weight loss was recorded at 310 °C, with 17% caused by the loss of $CO_2$ molecules from the polymeric backbone. A weight loss of 23.7% was



**Figure 7.** (a) DSC, (b) TGA and (c) derivative TG curves of PEG, PEG-NH$_2$, CMC, and grafted CMC-PEG.

**Table 2.** Thermal properties of CMC, PEG, PEG-NH$_2$ and grafted CMC-PEG.

| Polymers | $T_m^a$ [°C] | $\Delta H_m^a$ [J/g] | $T_d^b$ [°C] | $T_{max}^b$ [°C] | Char yield$^b$ [%] |
|---|---|---|---|---|---|
| CMC | – | – | 193.61 | 301.49 | 40.27 |
| PEG | 58.59 | 163.41 | 358.30 | 427.97 | 1.33 |
| PEG-NH$_2$ | 49.91 | 95.53 | 191.87 | 331.90 | 4.13 |
| Grafted CMC-PEG | 56.80 | 38.15 | 279.32 | 310.00 419.07 | 47.68 |

$^a$Melting temperature ($T_m$) and enthalpy change ($\Delta H_m$) were determined from DSC.
$^b$Decomposition temperature ($T_d$) at which 5% mass loss occurs and char yield is defined as the mass percent of residue at 500 °C were determined from TGA while maximum temperature ($T_{max}$) was determined from DTG curves.

recorded at 419.07 °C, indicating the thermal decomposition of grafted CMC-PEG. Based on TGA/DTG analysis, the grafting of PEG-NH$_2$ onto the CMC backbone was shown to improve the thermal stability of grafted CMC-PEG.

## 3.7. Cell cytotoxicity

Cell cytotoxicity of grafted CMC-PEG against NHDFs was quantitatively evaluated using MTS assay. The grafted CMC-PEG was dissolved to concentrations ranging from 0.00001 to 10 mg/ml followed by culturing with NHDFs for 24 h, as shown in Figure 8. The grafted CMC-PEG exhibited a non-cytotoxicity effect towards NHDF cells with percentage cell viability ranging between 100.99±7.35 to 98.97±5.74% for concentrations below 1 mg/ml. The grafted CMC-PEG with a concentration of 2 mg/ml
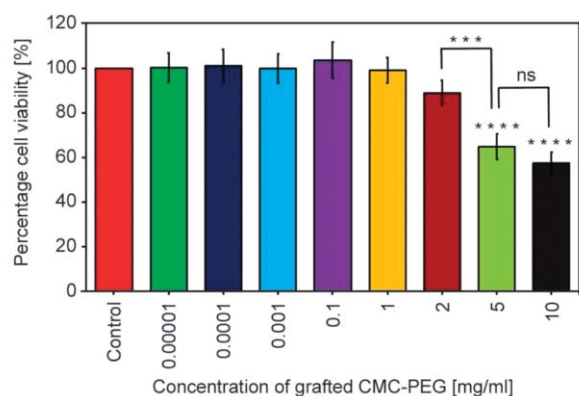


**Figure 8.** Cell viability of NHDFs after 24 h incubation (MTS assay) for grafted CMC-PEG with different concentrations ranging from 0.00001 to 10 mg/ml. Data with symbols are significantly different with $p > 0.05$ defined as ns, ***$p \leq 0.001$ and ****$p \leq 0.0001$.

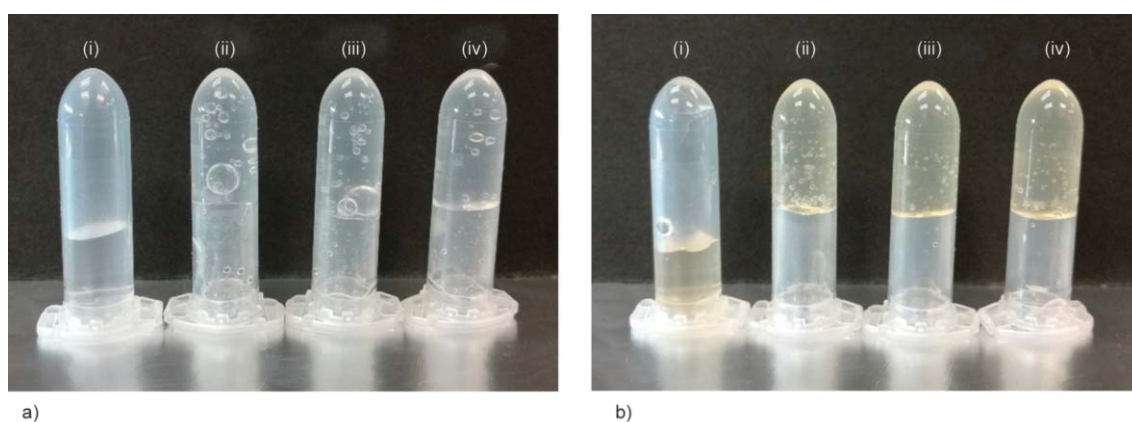showed a slight cytotoxic effect with 88.83±5.48% cell viability. Thereafter, the NHDFs viability reduced significantly with increasing concentrations of grafted CMC-PEG to 5 and 10 mg/ml. Based on the findings of the MTS assay, it can be concluded that the grafted CMC-PEG exhibited low cytotoxicity property and excellent biocompatibility for up to 2 mg/ml of grafted polymer concentration.

## 3.8. Rheological analysis

The citric acid (CA) crosslinked hydrogels formed through the formation of an ester bond between the –COOH groups of acid and –OH groups of polysaccharides. This process is known as esterification [48]. Therefore, CA could be used to chemically crosslinked the grafted CMC-PEG to form hydrogels. Then, a rheological analysis was conducted to study the rheological properties of the crosslinked hydrogels as hydrogel inks for 3D-bioprinting or injectable hydrogels. For example, the literature reported that the viscosity of extruding materials for extrusion-based 3D-bioprinting should be between 0.3 to 6000 Pa·s [49, 50]. This information could be useful for the development of hydrogels for specific biomedical applications. In this study, the sol-gel transition and flow behavior of CMC and grafted CMC-PEG crosslinked with CA was studied via tube inversion method as shown in Figure 9. An induced flow was observed for uncross-linked 2.5% (w/v) CMC and 10% (w/v) grafted CMC-PEG after tube inversion. This indicates that the samples were not able to maintain the shape, which could limit their potential for advanced biomaterials development [51]. On the other hand, CMC and grafted CMC-PEG formed



**Figure 9.** Photographs showing the flow behavior of (a) (i) uncross-linked 2.5% (w/v) CMC cross-linked, and 2.5% (w/v) CMC cross-linked with (ii) 5% (w/v), (iii) 10% (w/v) and (iv) 15% (w/v) CA and (b) (i) uncross-linked 10% (w/v) grafted CMC-PEG and 10% (w/v) grafted CMC-PEG crosslinked with (ii) 5% (w/v), (iii) 10% (w/v) and (iv) 15% (w/v) CA at 37 °C.

stable hydrogels upon the addition of 5, 10, and 15% (w/v) CA crosslinker, respectively. Based on the preliminary studies, 2.5% (w/v) CMC and 10% (w/v) grafted CMC-PEG crosslinked with 5% (w/v) CA exhibited shear-thinning behavior and viscosities suitable as injectable hydrogels and hydrogel inks for 3D-bioprinting. These formulations were subjected to further rheological analysis, such as strain-dependent and frequency-dependent studies.

Storage ($G'$) and loss ($G''$) moduli measure the extent to which a hydrogel can respond to stress by either absorb energy ($G'$) or undergo stress relation to dissipate the energy ($G''$) [52]. For strain-dependent and frequency-dependent studies, the chosen formulations of 2.5% (w/v) and 10% (w/v) grafted CMC-PEG cross-linked with 5% (w/v) CA, represented by 2.5% $CMC_5$ and 10% $CMC-PEG_5$ were studied. The purpose of the strain sweep was to determine the linear viscoelastic region (LVR) and mechanical properties of the crosslinked hydrogels. At low strain (<20%), the storage modulus ($G'$) and loss modulus ($G''$) of 2.5% (w/v) $CMC_5$ and 10% (w/v) $CMC-PEG_5$ were constant and parallel with $G' > G''$ indicating that the materials show a gel-like structure termed as viscoelastic solid material (Figure 10a). At high strain (>40%), the temporary structure of 10% $CMC-PEG_5$ was destroyed, and $G'$ started to decrease abruptly, whereas $G''$ started to increase, indicating deformation of the gel state [53]. The intersection of $G'$ and $G''$ of 10% (w/v) $CMC-PEG_5$ at 147% indicating the collapse of the gel state to a quasi-liquid state [54]. On the other hand, 2.5% (w/v) $CMC_5$ hydrogels exhibited viscoelastic fluid characteristics with $G' < G''$.

Figure 10b presents $G'$ and $G''$ of 2.5% (w/v) $CMC_5$ and 10% (w/v) $CMC-PEG_5$ hydrogels as a function of angular frequency ranging from 0.1 to 100 rad/s

at 0.5% strain. The frequency-dependent test measures the time-dependent viscoelastic properties of the crosslinked hydrogel network within the non-destructive LVR region [55]. The high frequency represents short-term behavior such as mixing and extruding; meanwhile, the low frequency indicates long-term behavior such as settling [56]. The 10% (w/v) CMC-PEG5 hydrogel exhibit a sharp increase of $G'$ at higher frequencies, indicating a 'solid-like' behavior predominates and gel stability due to the 3D structure of the crosslinked hydrogels. However, the G' of 2.5% (w/v) CMC5 hydrogel decreased abruptly at higher frequencies (G'<G'') with cross-over between $G'$ and $G''$ which indicates the viscoelastic liquid properties with undefined network structure. Based on the rheological studies, 10% (w/v) CMC-PEG5 hydrogel showed enhanced mechanical properties and promising rheological properties compared to 2.5% (w/v) CMC5 hydrogel.

## 4. Conclusions
In the present work, grafted CMC-PEG was successfully synthesized in the presence of EDC and NHS as the activators. FT-IR confirmed the amination of PEG and grafting of PEG-$NH_2$ to the CMC backbone through the formation of an amide bond. The successful grafting was also confirmed by ^{1}H NMR and solid-state ^{13}C CPMAS NMR due to the appearance of characteristic peaks around 7 and 174 ppm corresponded to the proton and carbon of the amide group. XRD findings of grafted CMC-PEG showed a semi-crystalline nature. Thermal studies by DSC further confirmed the semi-crystalline nature of grafted CMC-PEG, while TGA showed enhanced thermal stability compared to the polymer substrates. In vitro cytotoxicity assay confirmed the non-cytotoxic property of grafted CMC-PEG and excellent
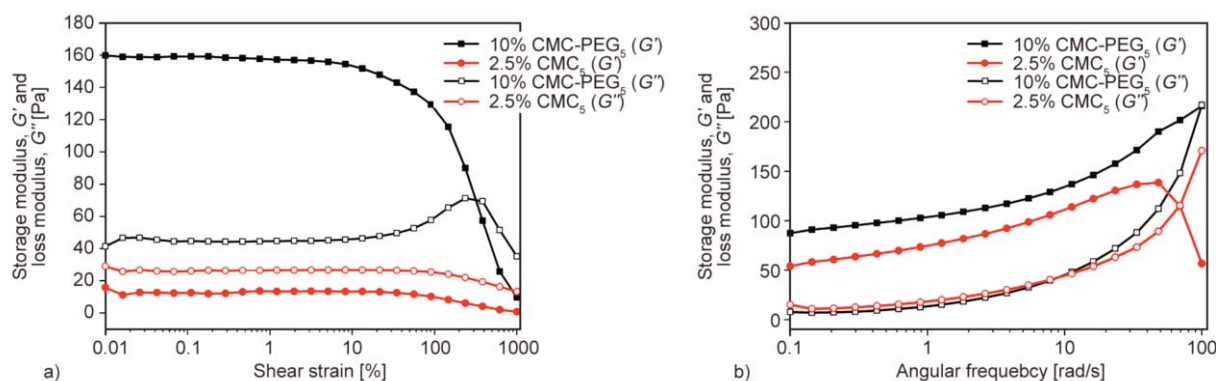


**Figure 10.** (a) Strain-dependent and (b) frequency-dependent oscillatory shear rheology of the hydrogels. *Hydrogels with subscript 5 indicate the 5% (w/v) percentage composition of CA in the crosslinked hydrogel samples.

biocompatibility with NHDFs. The rheological analysis reported that grafted CMC-PEG crosslinked with CA improved the hydrogel's viscosity. The further rheological analysis found 10% (w/v) grafted CMC-PEG crosslinked with 5% (w/v) CA to be the best hydrogel formulation with improved mechanical property compared to the CMC crosslinked with 5% (w/v) CA. The hydrogel of grafted CMC-PEG demonstrated potential use as hydrogel inks for 3D-bioprinting and injectable hydrogels for various biomedical applications such as tissue engineering, drug delivery system, and wound dressing materials.

## Acknowledgements

## References

[1] Hai T. A. P., Matsukuma H., Sugimoto R.: Grafting poly (3-hexylthiophene) to the surface of polypropylene using oxidative polymerization. Polymer, **121**, 247–255 (2017).
https://doi.org/10.1016/j.polymer.2017.06.027

[2] Wu C-S.: A comparison of the structure, thermal properties, and biodegradability of polycaprolactone/chitosan and acrylic acid grafted polycaprolactone/chitosan. Polymer, **46**, 147–155 (2005).
https://doi.org/10.1016/j.polymer.2004.11.013

[3] Vaidya A. A., Hussain I., Gaugler M., Smith D. A.: Synthesis of *graft* copolymers of chitosan-poly(caprolactone) by lipase catalysed reactive extrusion. Carbohydrate Polymers, **217**, 98–109 (2019).
https://doi.org/10.1016/j.carbpol.2019.03.081

[4] Kato K., Uchida E., Kang E-T., Uyama Y., Ikada Y.: Polymer surface with *graft* chains. Progress in Polymer Science, **28**, 209–259 (2003).
https://doi.org/10.1016/S0079-6700(02)00032-1

[5] Liu Y., Zhao K.: Rheological and dielectric behavior of milk/sodium carboxymethylcellulose mixtures at various temperatures. Journal of Molecular Liquids, **290**, 111175/1–111175/7 (2019).
https://doi.org/10.1016/j.molliq.2019.111175

[6] Fekete T., Borsa J., Takács E., Wojnárovits L.: Synthesis of carboxymethylcellulose/acrylic acid hydrogels with superabsorbent properties by radiation-initiated cross-linking. Radiation Physics and Chemistry, **124**, 135–139 (2016).
https://doi.org/10.1016/j.radphyschem.2015.09.018

[7] Candido R. G., Gonçalves A. R.: Synthesis of cellulose acetate and carboxymethylcellulose from sugarcane straw. Carbohydrate Polymers, **152**, 679–686 (2016).
https://doi.org/10.1016/j.carbpol.2016.07.071

[8] Kono H.: Characterization and properties of carboxymethyl cellulose hydrogels crosslinked by polyethylene glycol. Carbohydrate Polymers, **106**, 84–93 (2014).
https://doi.org/10.1016/j.carbpol.2014.02.020

[9] Ghorpade V. S., Yadav A. V., Dias R. J., Mali K. K., Pargaonkar S. S., Shinde P. V., Dhane N. S.: Citric acid crosslinked carboxymethylcellulose-poly (ethylene glycol) hydrogel films for delivery of poorly soluble drugs. International Journal of Biological Macromolecules, **118**, 783–791 (2018).
https://doi.org/10.1016/j.ijbiomac.2018.06.142

[10] Kumar B., Negi Y. S.: Water absorption and viscosity behaviour of thermally stable novel *graft* copolymer of carboxymethyl cellulose and poly(sodium 1-hydroxy acrylate). Carbohydrate Polymers, **181**, 862–870 (2018).
https://doi.org/10.1016/j.carbpol.2017.11.066

[11] Alange V. V., Birajdar R. P., Kulkarni R. V.: Novel spray dried pH-sensitive polyacrylamide-*grafted*-carboxymethylcellulose sodium copolymer microspheres for colon targeted delivery of an anti-cancer drug. Journal of Biomaterials Science, Polymer Edition, **28**, 139–161 (2017).
https://doi.org/10.1080/09205063.2016.1257083

[12] Dahlan N. A., Pushpamalar J., Veeramachineni A. K., Muniyandy S.: Smart hydrogel of carboxymethyl cellulose grafted carboxymethyl polyvinyl alcohol and properties studied for future material applications. Journal of Polymers and the Environment, **26**, 2061–2071 (2018).
https://doi.org/10.1007/s10924-017-1105-3

[13] Li H., Liu S., Lin L.: Rheological study on 3D printability of alginate hydrogel and effect of graphene oxide. International Journal of Bioprinting, **2**, 54–66 (2016).
https://doi.org/10.18063/IJB.2016.02.007

[14] Drury J. L., Mooney D. J.: Hydrogels for tissue engineering: Scaffold design variables and applications. Biomaterials, **24**, 4337–4351 (2003).
https://doi.org/10.1016/S0142-9612(03)00340-5

[15] Namazi H., Rakhshaei R., Hamishehkar H., Kafil H. S.: Antibiotic loaded carboxymethylcellulose/MCM-41 nanocomposite hydrogel films as potential wound dressing. International Journal of Biological Macromolecules, **85**, 327–334 (2016).
https://doi.org/10.1016/j.ijbiomac.2015.12.076

[16] Ghorpade V. S., Yadav A. V., Dias R. J.: Citric acid crosslinked β-cyclodextrin/carboxymethylcellulose hydrogel films for controlled delivery of poorly soluble drugs. Carbohydrate Polymers, **164**, 339–348 (2017).
https://doi.org/10.1016/j.carbpol.2017.02.005

[17] Lee S., Park Y. H., Ki C. S.: Fabrication of PEG–carboxymethylcellulose hydrogel by thiol-norbornene photo-click chemistry. International Journal of Biological Macromolecules, **83**, 1–8 (2016).
https://doi.org/10.1016/j.ijbiomac.2015.11.050

[18] Bang S., Ko Y-G., Kim W. I., Cho D., Park W. H., Kwon O. H.: Preventing postoperative tissue adhesion using injectable carboxymethyl cellulose-pullulan hydrogels. International Journal of Biological Macromolecules, **105**, 886–893 (2017).
https://doi.org/10.1016/j.ijbiomac.2017.07.103

[19] Gaihre B., Jayasuriya A. C.: Fabrication and characterization of carboxymethyl cellulose novel microparticles for bone tissue engineering. Materials Science and Engineering: C, **69**, 733–743 (2016).
https://doi.org/10.1016/j.msec.2016.07.060

[20] Cameron D. J. A., Bissessur R., Dahn D. C.: Synthesis and characterization of poly(ethylene glycol amine) electrolytes and nanocomposites based on graphite. European Polymer Journal, **48**, 1525–1537 (2012).
https://doi.org/10.1016/j.eurpolymj.2012.05.018

[21] Guler Z., Sarac A.: Electrochemical impedance and spectroscopy study of the EDC/NHS activation of the carboxyl groups on poly(ε-caprolactone)/poly(m-anthranilic acid) nanofibers. Express Polymer Letters, **10**, 96–110 (2016).
https://doi.org/10.3144/expresspolymlett.2016.11

[22] Kumar A., Sharma S., Kumar R.: The *graft* copolymerization of *N*-vinyl-2-pyrrolidone onto carboxymethyl cellulose and its application for controlled release of water-soluble levofloxacin. Journal of Polymer Research, **27**, 46/1–46/9 (2020).
https://doi.org/10.1007/s10965-020-2023-y

[23] Pettignano A., Charlot A., Fleury E.: Carboxyl-functionalized derivatives of carboxymethyl cellulose: Towards advanced biomedical applications. Polymer Reviews, **59**, 510–560 (2019).
https://doi.org/10.1080/15583724.2019.1579226

[24] Kumar D., Pandey J., Raj V., Kumar P.: A review on the modification of polysaccharide through *graft* copolymerization for various potential applications. The Open Medicinal Chemistry Journal, **11**, 109–126 (2017).
https://doi.org/10.2174/1874104501711010109

[25] Mahou R., Wandrey C.: Versatile route to synthesize heterobifunctional poly(ethylene glycol) of variable functionality for subsequent pegylation. Polymers, **4**, 561–589 (2012).
https://doi.org/10.3390/polym4010561

[26] Piegat A., Goszczyńska A., Idzik T., Niemczyk A.: The importance of reaction conditions on the chemical structure of N,O-acylated chitosan derivatives. Molecules, **24**, 3047/1–3047/16 (2019).
https://doi.org/10.3390/molecules24173047

[27] Kumar D., Rub M. A., Asiri A. M.: Synthesis and characterization of geminis and implications of their micellar solution on ninhydrin and metal amino acid complex. Royal Society Open Science, **7**, 200775/1–200775/13 (2020).
https://doi.org/10.1098/rsos.200775

[28] Baharifar H., Khoobi M., Bidgoli S. A., Amani A.: Preparation of PEG-grafted chitosan/streptokinase nanoparticles to improve biological half-life and reduce immunogenicity of the enzyme. International Journal of Biological Macromolecules, **143**, 181–189 (2020).
https://doi.org/10.1016/j.ijbiomac.2019.11.157

[29] Tan B., Huang Z., Yin Z., Min X., Liu Y., Wu X., Fang M.: Preparation and thermal properties of shape-stabilized composite phase change materials based on polyethylene glycol and porous carbon prepared from potato. RSC Advances, **6**, 15821–15830 (2016).
https://doi.org/10.1039/C5RA25685B

[30] Zhang X., Yao J., Zhang L., Fang J., Bian F.: Synthesis and characterization of PEG-conjugated quaternized chitosan and its application as a gene vector. Carbohydrate Polymers, **103**, 566–572 (2014).
https://doi.org/10.1016/j.carbpol.2013.12.072

[31] Badwaik H. R., Sakure K., Alexander A., Ajazuddin, Dhongade H., Tripathi D. K.: Synthesis and characterisation of poly(acrylamide) grafted carboxymethyl xanthan gum copolymer. International Journal of Biological Macromolecules, **85**, 361–369 (2016).
https://doi.org/10.1016/j.ijbiomac.2016.01.014

[32] Yang Y., Liu Y., Chen S., Cheong K-L., Teng B.: Carboxymethyl β-cyclodextrin grafted carboxymethyl chitosan hydrogel-based microparticles for oral insulin delivery. Carbohydrate Polymers, **246**, 116617/1–116617/9 (2020).
https://doi.org/10.1016/j.carbpol.2020.116617

[33] Takeshita H., Sasagawa G., Takenaka K., Miya M., Shiomi T.: Crystallization of *graft* copolymers 1. *Graft* chains miscible with main chains. Polymer Journal, **42**, 482–488 (2010).
https://doi.org/10.1038/pj.2010.24

[34] Sugiyama F., Kleinschmidt A. T., Kayser L. V., Rodriquez D., Finn M., Alkhadra M. A., Wan J. M-H., Ramírez J., Chiang A. S-C., Root S. E., Savagatrup S., Lipomi D. J.: Effects of flexibility and branching of side chains on the mechanical properties of low-bandgap conjugated polymers. Polymer Chemistry, **9**, 4354–4363 (2018).
https://doi.org/10.1039/C8PY00820E

[35] Ciftci M.: Synthesis of *graft* copolymers by combination of radical photopolymerization and iniferter process. Journal of Polymer Science Part A: Polymer Chemistry, **57**, 1344–1348 (2019).
https://doi.org/10.1002/pola.29395

[36] Dao T. P. T., Nguyen T. H., To V. V., Ho T. H., Nguyen T. A., Dang M. C.: A new formulation of curcumin using poly(lactic-*co*-glycolic acid)–polyethylene glycol diblock copolymer as carrier material. Advances in Natural Sciences: Nanoscience and Nanotechnology, **5**, 035013/1-035013/7 (2014).
https://doi.org/10.1088/2043-6262/5/3/035013

[37] Veeramachineni A. K., Sathasivam T., Muniyandy S., Janarthanan P., Langford S. J., Yan L. Y.: Optimizing extraction of cellulose and synthesizing pharmaceutical grade carboxymethyl sago cellulose from Malaysian sago pulp. Applied Sciences, **6**, 170/1–170/18 (2016).
https://doi.org/10.3390/app6060170

[38] Jiang W., Yang L., Qiu L., Xu J., Yang X., Wang J., Zhou H., Wang D.: Multifunctional hybrid nanoparticles based on sodium carboxymethylcellulose-*graft*-histidine and TPGS for enhanced effect of docetaxel. RSC Advances, **5**, 53835–53845 (2015).
https://doi.org/10.1039/C5RA05586E

[39] Capanema N. S., Mansur A. A., Mansur H. S., de Jesus A. C., Carvalho S. M., Chagas P., de Oliveira L. C.: Eco-friendly and biocompatible cross-linked carboxymethyl-cellulose hydrogels as adsorbents for the removal of organic dye pollutants for environmental applications. Environmental Technology, **39**, 2856–2872 (2018).
https://doi.org/10.1080/09593330.2017.1367845

[40] Li H-L., He Y-X., Gao Q-H., Wu G-Z.: Folate-polyethylene glycol conjugated carboxymethyl chitosan for tumor-targeted delivery of 5-fluorouracil. Molecular Medicine Reports, **9**, 786–792 (2014).
https://doi.org/10.3892/mmr.2014.1917

[41] Kono H.: 1H and 13C chemical shift assignment of the monomers that comprise carboxymethyl cellulose. Carbohydrate Polymers, **97**, 384–390 (2013).
https://doi.org/10.1016/j.carbpol.2013.05.031

[42] Dai H., Zhang Y., Ma L., Zhang H., Huang H.: Synthesis and response of pineapple peel carboxymethyl cellulose-*g*-poly (acrylic acid-co-acrylamide)/graphene oxide hydrogels. Carbohydrate Polymers, **215**, 366–376 (2019).
https://doi.org/10.1016/j.carbpol.2019.03.090

[43] Li J., Fang L., Tait W. R., Sun L., Zhao L., Qian L.: Preparation of conductive composite hydrogels from carboxymethyl cellulose and polyaniline with a nontoxic crosslinking agent. RSC Advances, **7**, 54823–54828 (2017).
https://doi.org/10.1039/C7RA10788A

[44] Goswami A., Bajpai A. K., Bajpai J., Sinha B. K.: Designing vanadium pentoxide-carboxymethyl cellulose/polyvinyl alcohol-based bionanocomposite films and study of their structure, topography, mechanical, electrical and optical behavior. Polymer Bulletin, **75**, 781–807 (2018).
https://doi.org/10.1007/s00289-017-2067-2

[45] Kwon S. K., Kim D. H.: Effect of process parameters of UV-assisted gas-phase cleaning on the removal of PEG (polyethyleneglycol) from a Si substrate. Journal Korean Physical Society, **49**, 1421–1427 (2006).

[46] Awada H., Daneault C.: Chemical modification of poly (vinyl alcohol) in water. Applied Sciences, **5**, 840–850 (2015).
https://doi.org/10.3390/app5040840

[47] Neto C. G. T., Giacometti J. A., Job A. E., Ferreira F. C., Fonseca J. L. C., Pereira M. R.: Thermal analysis of chitosan based networks. Carbohydrate Polymers, **62**, 97–103 (2005).
https://doi.org/10.1016/j.carbpol.2005.02.022

[48] Uranga J., Nguyen B. T., Si T. T., Guerrero P., de la Caba K.: The effect of cross-linking with citric acid on the properties of agar/fish gelatin films. Polymers, **12**, 291/1–291/12 (2020).
https://doi.org/10.3390/polym12020291

[49] Derakhshanfar S., Mbeleck R., Xu K., Zhang X., Zhong W., Xing M.: 3D bioprinting for biomedical devices and tissue engineering: A review of recent trends and advances. Bioactive Materials, **3**, 144–156 (2018).
https://doi.org/10.1016/j.bioactmat.2017.11.008

[50] He Y., Yang F., Zhao H., Gao Q., Xia B., Fu J.: Research on the printability of hydrogels in 3D bioprinting. Scientific Reports, **6**, 29977/1–29977/13 (2016).
https://doi.org/10.1038/srep29977

[51] Li H., Tan Y. J., Leong K. F., Li L.: 3D bioprinting of highly thixotropic alginate/methylcellulose hydrogel with strong interface bonding. ACS Applied Materials and Interfaces, **9**, 20086–20097 (2017).
https://doi.org/10.1021/acsami.7b04216

[52] Chen M. H., Wang L. L., Chung J. J., Kim Y-H., Atluri P., Burdick J. A.: Methods to assess shear-thinning hydrogels for application as injectable biomaterials. ACS Biomaterials Science and Engineering, **3**, 3146–3160 (2017).
https://doi.org/10.1021/acsbiomaterials.7b00734

[53] Ou K., Dong X., Qin C., Ji X., He J.: Properties and toughening mechanisms of PVA/PAM double-network hydrogels prepared by freeze-thawing and anneal-swelling. Materials Science and Engineering: C, **77**, 1017–1026 (2017).
https://doi.org/10.1016/j.msec.2017.03.287

[54] Gačanin J., Kovtun A., Fischer S., Schwager V., Quambusch J., Kuan S. L., Liu W., Boldt F., Li C., Yang Z., Liu D., Wu Y., Weil T., Barth H., Ignatius A.: Spatiotemporally controlled release of rho inhibiting C3 toxin from a protein–DNA hybrid hydrogel for targeted inhibition of osteoclast formation and activity. Advanced Healthcare Materials, **6**, 1700392/1–1700392/12 (2017).
https://doi.org/10.1002/adhm.201700392

[55] Zuidema J. M., Rivet C. J., Gilbert R. J., Morrison F. A.: A protocol for rheological characterization of hydrogels for tissue engineering strategies. Journal of Biomedical Materials Research Part B: Applied Biomaterials, **102**, 1063–1073 (2014).
https://doi.org/10.1002/jbm.b.33088

[56] Paxton N., Smolan W., Böck T., Melchels F., Groll J., Jungst T.: Proposal to assess printability of bioinks for extrusion-based bioprinting and evaluation of rheological properties governing bioprintability. Biofabrication, **9**, 044107/1–044107/18 (2017).
https://doi.org/10.1088/1758-5090/aa8dd8